Available online at www.sciencedirect.com
SCIENCE DIRECT
Carbohydrate Research 341 (2006) 1011–1019
Carbohydrate RESEARCH

Molecular dynamics simulations of a cyclic-β-(1→2) glucan containing an α-(1→6) linkage as a 'molecular alleviator' for the macrocyclic conformational strain

Hyunmyung Kim,[a] Karpjoo Jeong,[b] Kum Won Cho,[c] Seung R. Paik[d] and Seunho Jung[a,e,*]

[a]*Department of Bioscience and Biotechnology, Bio/Molecular Informatics Center, Konkuk University, 1 Hwayang-dong, Gwangjin-gu, Seoul 143-701, Republic of Korea*
[b]*College of Information and Communication, Bio/Molecular Informatics Center, Konkuk University, 1 Hwayang-dong, Gwangjin-gu, Seoul 143-701, Republic of Korea*
[c]*Supercomputing Application Technology Department, Supercomputing Center in Korea Institute of Science and Technology Information, Yusong-Gu, Eoeun-Dong 52, Daejon 305-806, Republic of Korea*
[d]*School of Chemical and Biological Engineering, Seoul National University, San 56-1, Shillim-Dong, Kwanak-Ku, Seoul 151-742, Republic of Korea*
[e]*Department of Microbial Engineering, Bio/Molecular Informatics Center, Konkuk University, 1 Hwayang-dong, Gwangjin-gu, Seoul 143-701, Republic of Korea*

Received 15 November 2005; received in revised form 18 February 2006; accepted 22 February 2006
Available online 20 March 2006

Abstract—The conformational preferences of a cyclic osmoregulated periplasmic glucan of *Ralstonia solanacearum* (OPGR), which is composed of 13 glucose units and linked entirely via β-(1→2) linkages excluding one α-(1→6) linkage, were characterized by molecular dynamics simulations. Of the three force fields modified for carbohydrates that were applied to select a suitable one for the cyclic glucan, the carbohydrate solution force field (CSFF) was found to most accurately simulate the cyclic molecule. To determine the conformational characteristics of OPGR, we investigated the glycosidic dihedral angle distribution, fluctuation, and the potential energy of the glucan and constructed hypothetical cyclic (CYS13) and linear (LINEAR) glucans. All β-(1→2)-glycosidic linkages of OPGR adopted stable conformations, and the dihedral angles fluctuated in this energy region with some flexibility. However, despite the inherent flexibility of the α-(1→6) linkage, the dihedral angles have no transition and are more rigid than that in a linear glucan. CYS13, which consists of only β-(1→2) linkages, is somewhat less flexible than other glycans, and one of its linkages adopts a higher energy conformation. In addition, the root-mean-square fluctuation of this linkage is lower than that of other linkages. Furthermore, the potential energy of glucans increases in the order of LINEAR, OPGR, and CYS13. These results provide evidence of the existence of conformational constraints in the cyclic glucan. The α-(1→6)-glycosidic linkage can relieve this constraint more efficiently than the β-(1→2) linkage. The conformation of OPGR can reconcile the tendency for individual glycosidic bonds to adopt energetically favorable conformations with the requirement for closure of the macrocyclic ring by losing the inherent flexibility of the α-(1→6)-glycosidic linkage.

Keywords: Molecular dynamic simulations; α-(1→6)-Glycosidic linkage; Cyclic osmoregulated periplasmic glucan; Macrocyclic ring constraint

1. Introduction

Many species of Gram-negative bacteria produce cyclic β-glucans that are sequestered in the periplasmic space. It has been proposed that an important function of these β-glucans is to maintain the osmotic potential of the periplasm, thereby enabling the bacterium to adapt to variations in the osmotic potential of its environment. These molecules also play a role in the phytopathogenicity of the bacteria.[1] The cyclic nature of these molecules could be essential for both aspects, and thus

* Corresponding author. Tel.: +82 2 450 3520; fax: +82 2 452 3611; e-mail: shjung@konkuk.ac.kr

0008-6215/$ - see front matter © 2006 Elsevier Ltd. All rights reserved.
doi:10.1016/j.carres.2006.02.025

a precise structural model is needed to assess these points.

Since a description of the cyclic all-β-(1→2) osmoregulated periplasmic glucans (OPGs) of Rhizobiaceae was first reported, there has been considerable interest in determining the structural features of these molecules, as their physiological function is assumed to be closely related to their conformation.[2–6] However, the conformational analysis of cyclic OPG is a challenging problem due to the high flexibility of the glycosidic linkages. This flexibility increases the entropic cost of crystallization, making it difficult to obtain crystals that are adequate for diffraction studies. Several conformational models for the cyclosophorans produced by Rhizobiaceae have been proposed on the basis of conformational energy calculations.[2–6]

Recently, the structures of two cyclic glucans extracted from cells of *Ralstonia solanacearum* and *Xanthomonas campestris* have been described.[7,8] These molecules share their cyclic nature with cyclosophorans of members of the Rhizobiaceae family. However, they are fundamentally different as a result of their unique degree of polymerization (DP, 13 vs 16 units) in contrast to the size distribution found in Rhizobiaceae, and by the presence of a single α-(1→6) linkage in contrast to the entirely β-(1→2) character of the OPGs found in the Rhizobiaceae members. The smallest cyclic glucan produced by Rhizobiaceae consists of a 17-residue macrocycle,[9] and smaller rings are apparently precluded by steric constraints.[2,8] However, the OPG of *Ralstonia* (OPGR) consists of 13 residues, which is smaller than the smallest cyclic glucan produced by Rhizobiaceae. Therefore, the conformation of OPGR should reconcile the tendency for individual glycosidic bonds to adopt an energetically favorable conformation with the requirement of closure of the macrocyclic ring.

In the present study, we have focused on the cyclic OPG of *R. solanacearum*, which, because of its small size (DP 13), is an ideal model to address the problems of potential cavities or other structural features that might be relevant for the function of these intriguing molecules. We performed molecular dynamics (MD) simulations on the OPG of *Ralstonia* (OPGR) in an aqueous environment. We compared the results with frequently used force fields for modeling of carbohydrates in an explicit solvent, namely GLYCAM, HGFB, and CSFF as applied to OPGR. CSFF showed excellent agreement with the reported experimental distances. Furthermore, we have investigated overall conformational characteristics and the patterns of several parameters that can express OPGR conformation. These analyses were carried out using the results obtained by MD simulations with CSFF. These data indicate that the α-(1→6) linkage of OPGR has some conformational rigidity, and this unusual rigidity can be explained by the closure of the macrocyclic ring.

2. Computational methods

The molecular model for the OPGR was built with the InsightII/Biopolymer program (version 2000, Accelrys, Inc. San Diego, USA). The glycosidic linkage of OPGR is described by two dihedral angles in the case of the β-(1→2) linkage: ϕ = H-1–C-1–O–C-2′ and ψ = C-1–O–C-2′–H-2′ and by three dihedral angles in the case of the α-(1→6) linkage: ϕ = O-5–C-1–O–C-6′, ψ = C-1–O–C-6′–C-5′ and ω = O–C-6′–C-5′–O-5′. Their two-dimensional molecular schemes and dihedral angles are presented in Figure 1. The initial coordinates of OPGR were determined using simulated annealing molecular dynamics (SA-MD), because their three-dimensional structures have not yet been identified.[6,10]

Simulations were performed using CHARMM 28B2[11] and AMBER-8.0[12] program packages with respective carbohydrate force fields. The older CHARMM-base force field (HGFB)[13] and the new generation of one (CSFF)[14] were used in CHARMM, and the most recent version of the AMBER-based force field (GLYCAM 04)[15] was used in AMBER. In these simulations, the temperature was

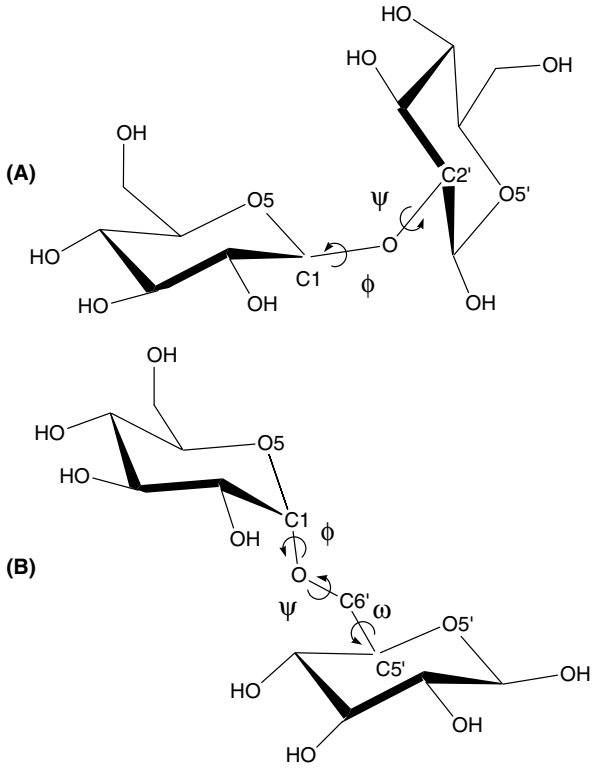

Figure 1. Schematic representation of glycosidic linkages in the cyclic osmoregulated periplasmic glucan of *Ralstonia solanacearum* (OPGR). The dihedral angle is marked with arrows. The glycosidic linkage of OPGR is described by two dihedral angles in the case of the β-(1→2) linkage (A): ϕ = H-1–C-1–O–C-2′ and ψ = C-1–O–C-2′–H-2′ and by the three dihedral angles in the case of the α-(1→6) linkage (B): ϕ = O-5–C-1–O–C-6′, ψ = C-1–O–C-6′–C-5′ and ω = O–C-6′–C-5′–O-5′. An α-(1→6) linkage has an additional glycosidic dihedral angle compared with the β-(1→2) linkage.

alternated between 300 and 1000 K 10 times. The total time for the SA-MD simulation was 30 ns. Ten structures were saved and fully energy minimized at the end of each production phase at 300 K, and the lowest-energy conformation among the 10 structures was selected for the initial structure of the subsequent SA-MD cycle.

The starting configurations of OPGR for the MD simulations in water were taken from the SA-MD conformations with the lowest-energy value. The geometries of the molecular models were fully optimized before the MD runs. A TIP3P three-site rigid water model[16] was used to solvate OPGR. Water molecules were removed if they were closer than 2.6 Å to any heavy atoms of OPGR. In summary, each system was constructed using periodic boundary conditions with a cubic box of dimensions 40 Å × 40 Å × 40 Å, consisting of OPGR and about 1600 water molecules. After this virtual solvation, the system was energy minimized for 1000 iterations. The MD simulations were performed in an isothermal–isobaric ensemble ($P = 1$ bar, $T = 298$ K), and the particle mesh Ewald summation method was used to treat the long-range electrostatic interactions.[17] The bond lengths of water molecules were constrained with the SHAKE algorithm[18] and the time step was 1.0 fs. The short-range non-bonded interactions were truncated with a 13-Å cutoff. The temperature and pressure of the system were regulated using the Langevin piston method in conjunction with Hoover's thermostat[19] in CHARMM and using isotropic position scaling in conjunction with Berendsen temperature coupling[20] in AMBER. The system was gradually heated to 298 K for 20 ps and equilibrated for 100 ps at this temperature. The production MD trajectory with one snapshot per 1.0 ps was collected for 1000 ps. All the dynamic simulations and trajectory analysis were performed on a computational Grid system, called MGrid (http://www.mgrid.or.kr), to process a large number of force-field calculations simultaneously. The MGrid system was designed to support remote execution, file transfers, and standard interface to legacy MPI (Message Passing Interface) applications to run successful MD simulations.

3. Results and discussion

3.1. Selection of a force field

The conformational behavior of OPGR was explored by a molecular dynamics simulation, using three different force fields. We compared molecular dynamics trajectories obtained in three force fields especially developed for the simulation of carbohydrates in aqueous solutions, two of which were implemented in the general molecular mechanics program CHARMM (HGFB[13] and the most recent CSFF[14]) and the last release of GLYCAM force field (GLYCAM 04[15]) implemented in AMBER. Lippens et al.[21] experimentally observed the interglycosidic H-1–H-2′ distances for every β-(1→2)-glycosidic bond of OPGR through the off-resonance ROESY method. Therefore, these distances were used for finding a suitable force field in this cyclic oligosaccharide. Figure 2 shows the average interglycosidic distance between the H1 atom of one residue and the H-2 atom of the next

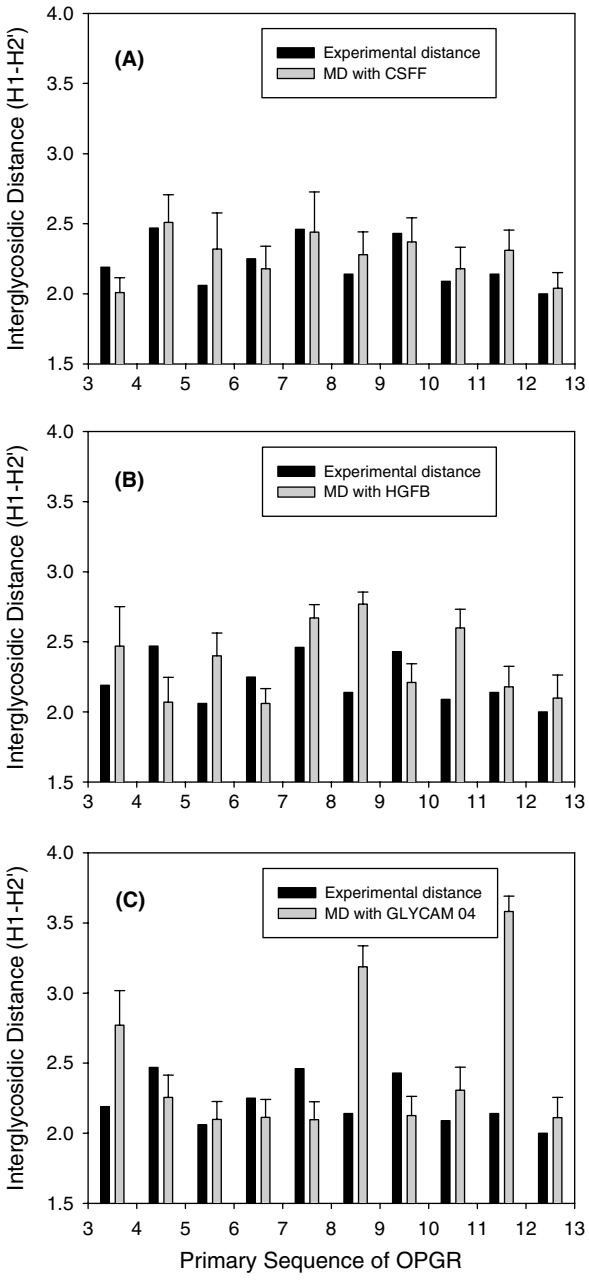

Figure 2. Comparison of the interglycosidic distance H-1–H-2′ (Å) along the primary sequence, resulting from experiments (off-resonance ROESY experiment[21]) and molecular dynamics simulations with several force fields; (A) CSFF in CHARMM; (B) HGFB in CHARMM; (C) GLYCAM 04 in AMBER. The primary sequence of glucose residues is shown in Figure 4.

residue in the trajectories of the MD simulations. The distances calculated from both the HGFB and GLYCAM force fields generally show higher values than the experimental distance, and the alternating pattern of the distance was also different. However, in the case of using the CSFF force field, the pattern and value of the interglycosidic distances are closely similar. Therefore, further analyses were conducted on MD simulations using CHARMM with CSFF.

According to the carbohydrate system and matter of interest in a given investigation, a certain force field will be more suitable than others. Although HGFB has known limitations, especially inaccurately modeled primary hydroxyl groups,[22] it has been demonstrated to reproduce a variety of experimental properties well.[23] The CSFF represents a second generation of the HGFB. This force field allows for conformationally representative simulations of (1→6)-linked saccharides in solution.[14] Furthermore, GLYCAM has been used for providing a quantitative explanation of the conformational behavior of a (1→6)-linked carbohydrate.[24] In the case of a cyclic oligosaccharide, CSFF is a more suitable force field when SA-MD and MD in an explicit solvent are used for the conformation search.

3.2. Conformational analysis of OPGR

Monosaccharides are generally assumed to have a rigid ring structure in conformation of an oligosaccharide.[25] Throughout the simulations, the $^4C_1$ ring form predom-

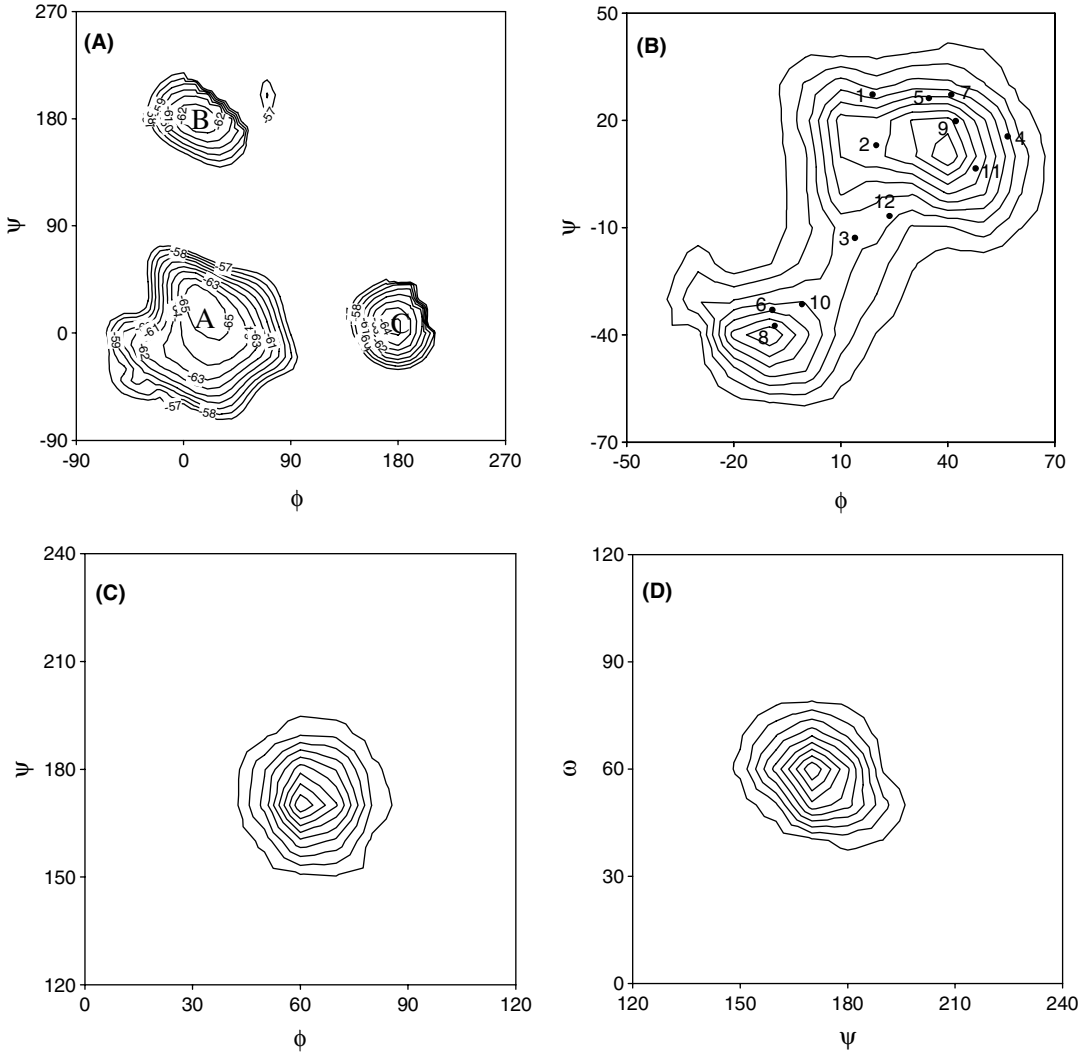

Figure 3. Calculated adiabatic potential-energy map for a disaccharide with a β-(1→2) linkage (A) and population density maps of the glycosidic dihedral angles from the molecular dynamics simulations of OPGR; (B) β-(1→2) linkage; (C) and (D) α-(1→6) linkage. The low-energy regions are specified A-, B-, and C-type regions,[8] and the contour lines correspond to 1 kcal/mol in (A). Contour lines correspond to the population densities of 10%, 20%, 30%, 40%, 50%, 60%, 70%, 80%, and 90% of the maximum value in (B)–(D). The Arabic numerals in (B) indicate the average dihedral angles between the n and $n+1$ residues of OPGR, and the primary sequence of glucose residues is shown in Figure 4. The scale of axes in (B)–(D) is confined to 120° for clear comparison.

inated for glucosyl moieties, as expected.[26] Therefore, characterizing the glycosidic linkages between the rigid monosaccharide units is the first step of a conformational analysis of oligosaccharides. An energetically favorable glycosidic bond conformation theoretically corresponds to residence in a well in the energy surface calculated as a function of various geometric parameters. The ϕ–ψ potential-energy map of the β-(1→2)-glycosidic linkage of two glucose residues is shown in Figure 3A. The ϕ and ψ glycosidic dihedral angles were defined as $\phi = (\text{H-1–C-1–O–C-2}')$ and $\psi = (\text{C-1–O–C-2}'\text{–H-2}')$ in the β-(1→2)-glycosidic linkage. The energy contour shows three major low-energy regions, A-, B-, and C-type, as reported by Mimura et al.[27] and by York[8] for sophorose from a rigid-residue Monte Carlo sampling analysis and by Dowd et al.,[28] who used an MM3 potential function.

In order to explore the conformational patterns, the population density map of glycosidic dihedral angles, ϕ and ψ, was generated for the trajectories of MD simulations. Figure 3B shows that all of the β-(1→2)-glycosidic dihedral angles of OPGR adopt the A-type conformation positioned in the lowest energy region of the potential-energy map. The A-type conformation is consistent with the conformation of the crystalline form of sophorose hydrate.[26] In the case of the α-(1→6) linkage, the ϕ, ψ, and ω glycosidic dihedral angles were defined as $\phi = (\text{O-5–C-1–O–C-6}')$, $\psi = (\text{C-1–O–C-6}'\text{–C-5}')$ and $\omega = (\text{O–C-6}'\text{–C-5}'\text{–O-5}')$, respectively. Figure 3 (Panels C and D) shows the population density map of the α-(1→6) linkage in MD simulations. One represents the same geometry of the α-(1→6) linkage that can be found in the crystal structure of α-panose[29] ($\phi = 71°$, $\psi = 165°$, $\omega = 76°$). The average values of the torsion angles ϕ, ψ, and ω in trajectories are $\langle\phi\rangle = 69°$, $\langle\psi\rangle = 177°$, and $\langle\omega\rangle = 63°$, respectively.

Because of the cyclic nature of cyclic glucans, these molecules require closure of the macrocyclic ring. York[8] has suggested that ring closure (steric constraint) in a β-(1→2)-cyclic glucan may be achieved by interrupting a perfectly alternating $^{+}$A^{-}A pattern of linkage conformations with two 'frame shifts' at which the alternating pattern is broken. The region of the energy well A wherein $\psi > -20°$ is defined as conformation $^{+}$A, and the region wherein $\psi < -20°$ is defined as conformation $^{-}$A according to York.[8] However, in our previous studies of cyclic β-(1→2) glucans composed of 17 and 21 glucose units, we could not find any alternating pattern and more than one linkage adopted B- and C-type conformation.[6,10] The somewhat high-energy B- and C-type conformations might relieve the macrocyclic ring constraint of a β-(1→2)-cyclic glucan.

However, the α-(1→6) linkage has additional flexibility and an independent coordinate associated with the extra degree of freedom. Because of the additional flexibility and independent coordinate associated with the

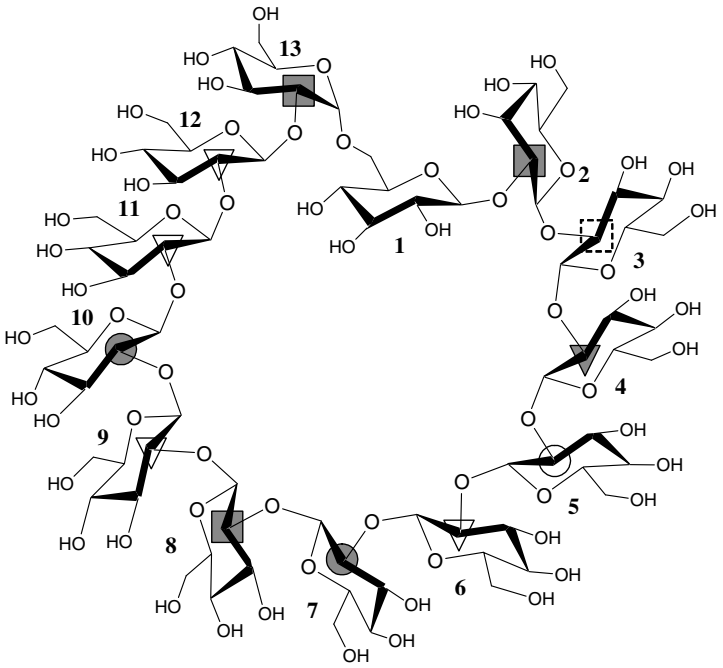

Figure 4. Comparison of the segmental flexibility between experimental (exchange contribution, Δ_{ex}) and theoretical (root-mean-square fluctuation (RMSF) results for the ψ angle in β-(1→2) linkages) for every residue of a cyclic glucan. The symbols represent exchange contributions to the relaxation of the C-2 nucleus. Squares represent exchange contributions $\Delta_{ex} < 10$ Hz, triangles correspond to $\Delta_{ex} = 20$–30 Hz, and circles correspond to $\Delta_{ex} > 50$ Hz.[34] Gray, open, and broken symbols represent good, some, and no agreement of segmental flexibility between the experimental and theoretical results, respectively. For details, refer to the text.

extra degree of freedom of the (1→6) linkage, no attempt was made to prepare a two-dimensional map for this linkage.[23] York[8] suggested that the α-(1→6) linkage can provide the topological reversal site that is required for closure of the macrocycle in the study of the cyclic OPG of *Xanthomonas*, which consists of 16 glucose residues with one α-(1→6) and other β-(1→2) linkages. Accordingly, all other β-(1→2) linkages of OPGR can exist at the lowest energy of conformation and are not trapped in either the B- or C-type, as shown in Figure 3B.

3.3. Characteristics of the α-(1→6) linkage in cyclic glucans

In general, (1→6) linkages are considered to be more flexible than other glycosidic linkages owing to the additional dihedral degree of freedom. For this reason, several transitions of the dihedral angles of the (1→6) linkage were observed in glucopyranose monomer, dimer, and oligomer,[14,24,30] and the sterically allowed region of a (1→6)-linked disaccharide occupies about twice the area compared to (1→2)-, (1→3)-, and (1→4)-linked disaccharides in the ϕ–ψ map.[31] Concerning the ω-dihedral angle, there are three possible staggered conformations being denoted by the standard notation *gg*, *gt*, and *tg* (corresponding to angles 300°, 60°, 180°, respectively), and these conformational transitions are on the order of nanoseconds.[14,24,30] However, in the case of OPGR, the dihedral angles of the α-(1→6) linkage adopts the *gg* conformation and has no transition up to 5 ns simulation time. This limited conformational diversity can be introduced by the interaction with other residues in vicinity of the α-(1→6) linkage of a branched glucan.[32] Cyclic glucans can hold an additional limited conformational diversity derived from macrocyclic ring constraint. Thus the conformation of the α-(1→6) linkage might be restricted to a *gg* type to minimize the macrocyclic constraint in the major β-(1→2) linkages of OPGR. Therefore, β-(1→2) linkages might be flexible and of the lowest energy conformation (A-type).

The approach to the investigation of dynamical properties in biomolecules is by means of heteronuclear relaxation measurements.[33] Figure 4 shows the experimental exchange contribution to the relaxation of the C-2 nucleus[34] and root-mean-square fluctuation (RMSF) of the ψ angle in β-(1→2) according to MD simulations. The considerable amount of the chemical exchange contributions reflects segmental flexibility and the existence of slow conformational exchange.[35,36] The RMSF of the ψ angle of the β-(1→2) linkage (C-1–O–C-2′–H-2′) was used as a parameter to compare the MD result with this experimental data. The values of the exchange contribution and RMSF were divided into three groups, High, Medium, and Low, denoted as H, M, and L, respectively, and these are provided in Table 1. The degree of agreement between the experimental and theoretical results are expressed as good, some, or no agreement, and is given for the set between the same symbols, M and others, or H and L, respectively. On the whole, the theoretical results correspond well with the experimental results. Furthermore, the exchange contribution and RMSF show low values around the α-(1→6) linkage, which links between 1 and 13 residues. The rigid nature of the α-(1→6) linkage and the flexible and low-energy conformation of the β-(1→2) linkages reveal the characteristics of cyclic osmoregulated periplasmic glucans of *Ralstonia* (OPGR).

Table 1. Comparison of the segmental flexibility between experimental (Δ_{ex}) and theoretical (root-mean-square fluctuation (RMSF) of the ψ angle in β-(1→2) linkages) results for every residue of cyclic glucan

Residue	2	3	4	5	6	7
Δ_{ex}[a]	L	L	M	H	M	H
OPGR[b]	L	H	M	M	L	H
CYS13[b]	L	L	L	L	L	L
Residue	8	9	10	11	12	13
Δ_{ex}[a]	L	M	H	M	M	L
OPGR[b]	L	L	H	L	H	L
CYS13[b]	L	L	M	L	L	M

[a] The symbols represent exchange contributions to the relaxation of the C-2 nucleus. L represents exchange contributions $\Delta_{ex} < 10$ Hz, M corresponds to $\Delta_{ex} = 20$–30 Hz, and H corresponds to $\Delta_{ex} > 50$ Hz.[34]

[b] The symbols represent RMSF of the ψ angle at each residue of cyclic glucans. L represents RMSF < 10°, M corresponds RMSF = 10°–13°, and H corresponds RMSF > 13°.

To investigate more detailed characteristics of the α-(1→6)-glycosidic linkage, we constructed a molecular model of a hypothetical cyclic glucan (CYS13) that consists of only β-(1→2) linkages. CYS13 has the same molecular weight, glucopyranosyl component, and linkage pattern as those of OPGR except for the presence of a single α-(1→6)-glycosidic bond. In addition to CYS13, we also constructed a linear glucan (LINEAR) containing a α-(1→6) linkage at the middle point while the remaining are β-(1→2) linkages (Fig. 5). In the case of CYS13, there is one B-type conformation that has a lower RMSF value than other linkages, and the values are 7.2 and 9.2, respectively. This result is similar to those from our previous studies.[6,10] The B-type conformation of the β-(1→2) linkage could adopt a somewhat unstable and rigid conformation that might relieve the macrocyclic ring constraint, which allows other linkages to be stable and flexible A-type conformations. However, some restraint remains, as indicated by the finding that the RMSF of the ψ-angle of most residues in CYS13 are lower than that of β-(1→2)-linked residues in OPGR (Table 1). In the case of LINEAR, the dihedral angles of the linkage are more flexible than OPGR. RMS fluctuations of the ϕ, ψ, and ω dihedral angles in the α-(1→6) linkage are 10.7, 13.4, and 9.0 in LINEAR and 8.9, 9.7,

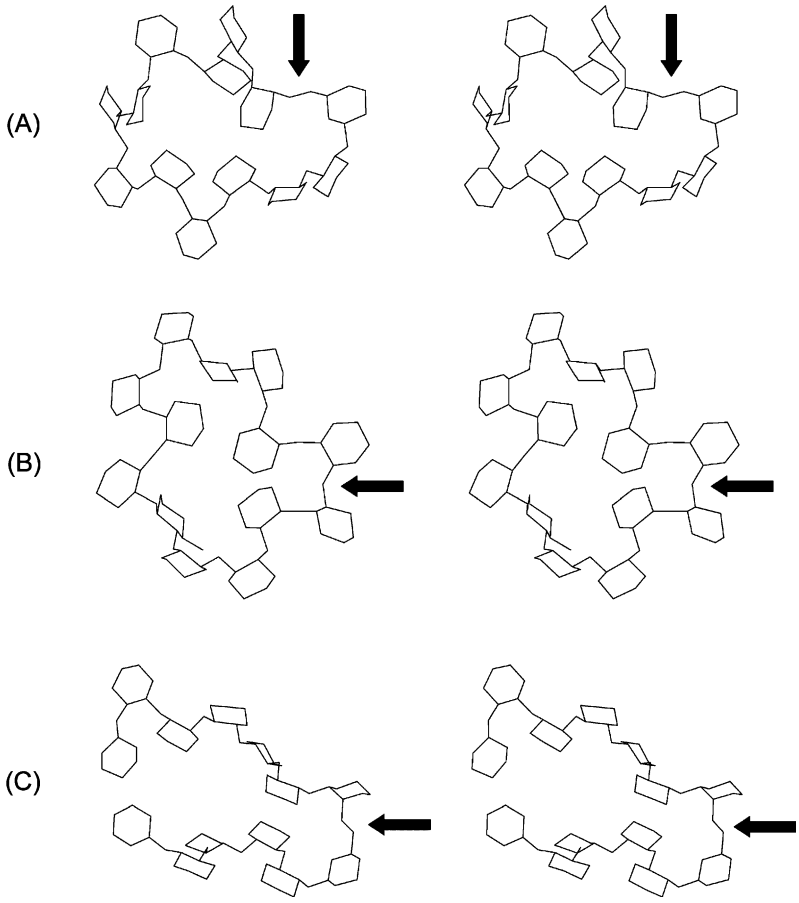

Figure 5. Stereoview of a representative conformation from the MD simulations; (A) OPGR; (B) CYS13; (C) LINEAR. All exocyclic groups have been omitted for clarity. Arrows indicate the α-(1→6) and β-(1→2) linkages that can induce a topologically reversal part.

and 8.8 in OPGR, respectively. Furthermore, β-(1→2) linkages of LINEAR are more flexible than those of cyclic glucans and adopt a stable A-type conformation. These results show the fact that LINEAR does not need any constraint to close the macrocyclic ring.

Figure 6 shows the moving average of potential energy for each glucan. Given a frame, the moving average is defined in a frame by taking the average of 101 frames in a range of 50 frames before and after that frame. LINEAR, which has no ring constraint, shows the lowest potential energy. In cyclic glucans, OPGR has lower potential energy than CYS13. These results can be explained by the finding that some ring constraints remain in cyclic glucans, and the α-(1→6) linkage of OPGR can relieve the constraint more efficiently than the B-type conformation of the β-(1→2) linkage of CYS13. These linkages act as a molecular alleviator, which reduces the macrocyclic ring constraint in cyclic glucans.

Representative conformations of the simulated glucans are shown in Figure 5. The conformation of OPGR and CYS13 is irregular without a large cavity. The topologically reversal parts can be induced by a certain linkage indicated by arrows [the α-(1→6) linkage in OPGR and LINEAR or the β-(1→2) linkage with B-type conformation in CYS13]. OPGR and LINEAR adopt a moderate turn around the α-(1→6) linkage and CYS13

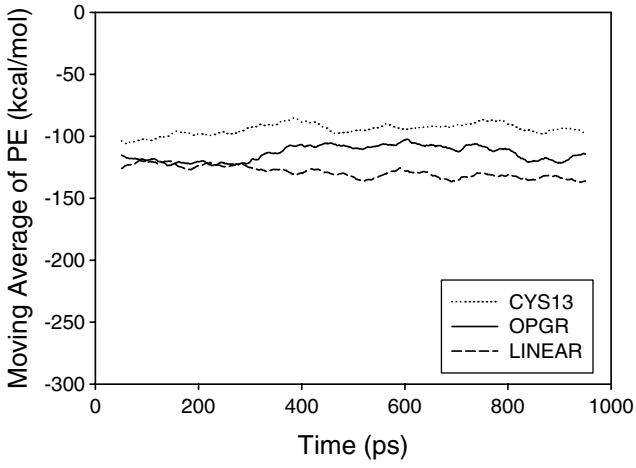

Figure 6. Moving average of potential energy (PE) of each glucan. Given a frame, the moving average is defined in a frame by taking the average of 101 frames in a range of 50 frames before and after that frame.

adopts a sharp turn around the β-(1→2) linkage. Both the distance between end residues and the overall length of LINEAR are shorter than those of another linear glucan that contains entirely β-(1→2)-glycosidic linkages (data not shown).

4. Conclusions

In this study, MD simulations were exploited to provide insight on the conformational features of the osmoregulated periplasmic glucan of *R. solanacearum* (OPGR). CSFF was more consistent with an alternative pattern of pairwise interglycosidic distances than the HGFB and GLYCAM 04 force fields when SA-MD and MD in explicit solvent are used for the conformation search. All β-(1→2)-glycosidic linkages of OPGR adopt stable conformations, and the ϕ and ψ dihedral angles fluctuate in this energy region with some flexibility. However, despite the inherent flexibility of the α-(1→6) linkage, the dihedral angle has no transition and shows rigidity during the MD simulation. On the whole, the exchange contribution and root-mean-square fluctuation of the ψ angle in β-(1→2) linkages show low values around the α-(1→6) linkages. CYS13, which consists of only β-(1→2) linkages, has less flexible glycosidic conformations than that of other glycans. One of its linkages adopts a somewhat higher energy conformation and is less flexible than that of other linkages. Furthermore, the potential energy of glucans increases in the order of LINEAR, OPGR, and CYS13. These results provide evidence for the existence of conformational constraints of cyclic glucan and an α-(1→6)-glycosidic linkage can alleviate this constraint more efficiently than a β-(1→2) linkage via loss of its inherent flexibility. The α linkages are considered relatively flexible in comparison with β linkages from oligosaccharides, and furthermore, a (1→6) linkage is more dynamic than other linkages.[31,37] However, in cyclic oligosaccharides, the α-(1→6) linkage shows the rigidity, which affects the conformation of the cyclic glucan, suggesting that it acts as a molecular alleviator for those macrocyclic conformational strains. These studies therefore provide a relationship between the function of specific glycosidic linkages and the segmental or overall conformation of glucans.

Acknowledgements

This study was supported by a grant of the MOST (Ministry of Science and Technology) through *e*-Science project of KISTI (Korea Institute of Science and Technology Information) and partially supported by a national R&D project in MOST for Biodiscovery in Korea, SDG.

References

1. Miller, K. J.; Kennedy, E. P.; Reinhold, V. N. *Science* **1986**, *231*, 48–51.
2. Palleschi, A.; Crescenzi, V. *Gazz. Chim. Ital.* **1985**, *115*, 243–245.
3. Poppe, L.; York, W. S.; van Halbeek, H. *J. Biomol. NMR* **1993**, *3*, 81–89.
4. York, W. S.; Thomson, J. U.; Meyer, B. *Carbohydr. Res.* **1993**, *248*, 55–80.
5. André, I.; Mazeau, K.; Taravel, F. R.; Tvaroska, I. *Int. J. Biol. Macromol.* **1995**, *17*, 189–198.
6. Kim, H.; Jeong, K.; Lee, S.; Jung, S. J. *Comput. Aided Mol. Des.* **2002**, *16*, 601–610.
7. Talaga, P.; Stahl, B.; Wieruszeski, J.-M.; Dillenkamp, F.; Tsuyumu, S.; Lippens, G.; Bohin, J. P. *J. Bacteriol.* **1996**, *178*, 2263–2271.
8. York, W. S. *Carbohydr. Res.* **1995**, *278*, 205–225.
9. Breedveld, M. W.; Miller, K. J. *Microbiol. Rev.* **1994**, *58*, 145–161.
10. Choi, Y.-H.; Yang, C.-H.; Kim, H.-W.; Jung, S. *Carbohydr. Res.* **2000**, *326*, 227–234.
11. Brooks, B. R.; Bruccoleri, R. E.; Olafson, B. D.; States, D. J.; Swaminathan, S.; Karplus, M. *J. Comput. Chem.* **1983**, *4*, 187–217.
12. Case, D. A.; Darden, T. A.; Cheatham, III, T. E.; Simmerling, C. L.; Wang, J.; Duke, R. E.; Luo, R.; Merz, K. M.; Wang, B.; Pearlman, D. A.; Crowley, M.; Brozell, S.; Tsui, V.; Gohlke, H.; Mongan, J.; Hornak, V.; Cui, G.; Beroza, P.; Schafmeister, C.; Caldwell, J. W.; Ross, W. S.; Kollman P. A. AMBER 8, University of California, San Francisco, 2004.
13. Ha, S. N.; Giammona, A.; Field, M.; Brady, J. W. *Carbohydr. Res.* **1988**, *180*, 207–221.
14. Kuttel, M.; Brady, J. W.; Naidoo, K. J. *J. Comput. Chem.* **2002**, *23*, 1236–1243.
15. Woods, R. J.; Dwek, R. A.; Edge, C. J.; Fraser-Reid, B. *J. Phys. Chem.* **1995**, *99*, 3832–3846.
16. Jorgensen, W. L. *J. Chem. Phys.* **1982**, *77*, 4156–4163.
17. Darden, T.; York, D.; Pedersen, L. *J. Chem. Phys.* **1993**, *98*, 10089–10092.
18. Ryckaert, J. P.; Ciccotti, G.; Berendsen, H. J. C. *J. Comput. Phys.* **1977**, *23*, 327–341.
19. Feller, S. E.; Zhang, Y.; Pastor, R. W.; Brooks, B. R. *J. Chem. Phys.* **1995**, *103*, 4613–4621.
20. Berendsen, H. J. C.; Postma, J. P. M.; van Gunsteren, W. F.; Dinola, A.; Haak, J. R. *J. Chem. Phys.* **1984**, *81*, 3684–3690.
21. Lippens, G.; Wieruszeski, J.-M.; Talaga, P.; Bohin, J.-P.; Desvaux, H. *J. Am. Chem. Soc.* **1996**, *118*, 7227–7228.
22. Kouwijzer, M. L. C. E.; van Eijck, B. P.; Kroes, S. J.; Kroon, J. *J. Comput. Chem.* **1993**, *14*, 1281–1289.
23. Naidoo, K. J.; Denysyk, D.; Brady, J. W. *Protein Eng.* **1997**, *10*, 1249–1261.
24. Kirschner, K. N.; Woods, R. J. *Proc. Natl. Acad. Sci. U.S.A.* **2001**, *98*, 10541–10545.
25. Wormald, M. R.; Petrescu, A. J.; Pao, Y.-L.; Glithero, A.; Elliott, T.; Dwek, R. A. *Chem. Rev.* **2002**, *102*, 371–386.
26. Ohanessian, P. J.; Longchambon, F.; Arene, F. *Acta Crystallogr., Sect. B* **1978**, *34*, 3666–3671.
27. Mimura, M.; Kitamura, S.; Cotoh, S.; Takeo, K.; Urakawa, H.; Jajiwara, K. *Carbohydr. Res.* **1996**, *289*, 25–37.
28. Dowd, M. K.; French, A. D.; Reilly, P. J. *Carbohydr. Res.* **1992**, *233*, 15–34.
29. Imberty, A.; Pérez, S. *Carbohydr. Res.* **1988**, *181*, 41–55.

30. Palleschi, A.; Bocchinfuso, G.; Coviello, T.; Alhaique, F. *Carbohydr. Res.* **2005**, *340*, 2154–2162.
31. Sathyanarayana, B. K.; Stevens, E. S. *J. Biomol. Struct. Dyn.* **1983**, *1*, 947–959.
32. Corzana, F.; Motawia, M. S.; du Penhoat, F.; van den Berg, F.; Blennow, A.; Pérez, S.; Egelsen, S. B. *J. Am. Chem. Soc.* **2004**, *126*, 13144–13155.
33. Palmer, A. G.; Williams, J.; McDermott, A. *J. Phys. Chem.* **1996**, *100*, 13293–13310.
34. Lippens, G.; Wieruszeski, J.-M.; Horvath, D.; Talaga, P.; Bohin, J.-P. *J. Am. Chem. Soc.* **1998**, *120*, 170–177.
35. Buck, M.; Boyd, J.; Redfield, C.; MacKenzie, D. A.; Jeenes, D. J.; Archer, D. B.; Dobson, C. M. *Biochemistry* **1995**, *34*, 4041–4055.
36. Renisio, J.; Pérez, J.; Czisch, M.; Guenneugues, M.; Bornet, O.; Frenken, L.; Cambillau, C.; Darbon, H. *Proteins* **2002**, *47*, 546–555.
37. Almond, A. *Carbohydr. Res.* **2005**, *340*, 907–920.